Shedding light on species boundaries in small endogeic animals through an integrative approach: species delimitation in the centipede *Clinopodes carinthiacus* (Chilopoda: Geophilidae) in the south-eastern Alps

EMILIANO PERETTI[1,*], CHIARA CECCHIN[2], GIUSEPPE FUSCO[1], LUCA GREGNANIN[1], IVAN KOS[3] and LUCIO BONATO[1]

[1]*Dipartimento di Biologia, Università di Padova, via Ugo Bassi 58B, I-35131 Padova, Italy*
[2]*Biocenter, Faculty of Biology, Ludwig-Maximilians-Universität, Großhaderner Strasse 2, 82152 Planegg-Martinsried, Germany*
[3]*Department of Biology, Biotechnical Faculty, University of Ljubljana, Večna pot 111, 1000 Ljubljana, Slovenia*

The investigation of species boundaries in strictly endogeic animals is challenging because they are prone to fine-scale genetic and phenotypic geographical differentiation owing to low dispersal ability. An integrative approach exploiting different sources of information has seldom been adopted in these animals and even more rarely by treating all data sources equally. We investigated species boundaries in the endogeic centipede *Clinopodes carinthiacus* across the south-eastern Alps by studying genetic and morphological differentiation in a sample of 66 specimens from 27 sites, complemented by the morphological examination of more than 1100 specimens from other sites. Hypotheses of species delimitation were obtained independently from the molecular sequences of three markers (mitochondrial 16S and *COI* and nuclear 28S) by means of different species discovery methods (automatic barcode gap discovery, assemble species by automatic partitioning, general mixed Yule coalescent and the Poisson tree process) and from ten morphological characters by means of a model-based cluster analysis and Bayesian model selection. We found strong support for the existence of at least two species: *C. carinthiacus s.s.* and *Clinopodes strasseri*, which was formerly described as a subspecies of another species, and later placed in synonymy with *C. carinthiacus*. The two species coexist in syntopy in at least one site.

ADDITIONAL KEYWORDS: Geophilomorpha – integrative taxonomy – soil invertebrates.

INTRODUCTION

Soil-dwelling animals contribute substantially to taxonomic and functional global biodiversity (e.g. Bardgett & van der Putten, 2014; Orgiazzi *et al.*, 2016). However, the magnitude and patterns of fine-scale geographical differentiation in these animals remain very uncertain and difficult to assess (e.g. Padial *et al.*, 2010; Carstens *et al.*, 2013). Species delimitation is especially challenging when aiming to discriminate species-level diversity from between-population variation in small, strictly endogeic animals that spend their entire life in the soil matrix. Owing to their low vagility and dispersal ability, these animals often show remarkable genetic differentiation among populations, associated with variable levels of phenotypic differentiation, from overall uniformity to micro-allopatric variation for traits under selection or drift (e.g. Rueffler *et al.*, 2006; Nosil *et al.*, 2009; Emerson *et al.*, 2011; Richardson *et al.*, 2014). When considering soil-dwelling animals, it is generally acknowledged that morphology-only investigations often underestimate the geographical turnover of species, whereas molecular-only taxonomy can overestimate it, and this discrepancy is expected to be exacerbated in strictly endogeic animals of small size (e.g. Bond & Stockman, 2008; Inäbnit *et al.*, 2019).

*Corresponding author. Email: emiliano.peretti@gmail.com

Integrative taxonomy (e.g. Dayrat, 2005; Will *et al.*, 2005; Padial *et al.*, 2010; Schlick-Steiner *et al.*, 2010) has emerged over the last 15 years as the gold standard in providing better-supported species delimitation hypotheses by reconciling the information from different lines of evidence (for details on the species concept underlying this approach, see De Queiroz, 1998, 2007; Hausdorf, 2011; Zachos, 2016). The integrative approach has repeatedly been advocated as theoretically more sound than single-evidence approaches, and it has also proved to be more effective in practice (Ezard *et al.*, 2010; Guillot *et al.*, 2012; Edwards & Knowles, 2014; Solís-Lemus *et al.*, 2015).

Nevertheless, the application of integrative taxonomy to small endogeic animals is still underexploited, especially when compared with other subjects of study, such as larger or epigeic animals. Among the few studies in which a type of integrative methodology was applied to endogeic animals, most were on free-living Nematoda (e.g. Gutiérrez-Gutiérrez *et al.*, 2010, 2013; Archidona-Yuste *et al.*, 2016; Powers *et al.*, 2016; Olson *et al.*, 2017) and Oligochaeta (e.g. Marchán *et al.*, 2018, 2020; Rota *et al.*, 2018) and a few others concerned endogeic lineages of Acari (Heethoff *et al.*, 2011), Pseudoscorpiones (Ohira *et al.*, 2018), Opiliones (Derkarabetian & Hedin, 2014), Oniscidea (Bedek *et al.*, 2019), Collembola (Sun *et al.*, 2017; Zhang *et al.*, 2018), Zygentoma (Espinasa & Giribet, 2009; Espinasa *et al.*, 2016) and Coleoptera (Pérez-González *et al.*, 2018). In nearly all these studies, a 'primary' hypothesis of species delimitation was first drawn from one type of data (usually molecular data), whereas other sources of information (usually morphological data) were used only to test further or corroborate the primary hypothesis. In other words, different sources of information were exploited in sequential steps of 'species discovery' and 'species validation' (Carstens *et al.*, 2013).

Despite multivariate statistical methodologies having been developed to draw hypotheses of species boundaries from morphological differentiation independently of molecular-based hypotheses and without a priori assumptions on the number of species (Ezard *et al.*, 2010; Guillot *et al.*, 2012; Edwards & Knowles, 2014; Cadena *et al.*, 2018), such methods have never been applied to strictly endogeic animals and rarely to other soil animals (e.g. Eberle *et al.*, 2016; Noguerales *et al.*, 2018). This contrasts with the approach used in the analysis of molecular data, where a diverse array of methods is often used to produce a set of species delimitation hypotheses independently of preliminary taxonomic hypotheses (e.g. Camargo & Sites, 2013; Carstens *et al.*, 2013; Flot, 2015).

Here, we take an integrative taxonomic approach to an endogeic animal across a broad, heterogeneous region. The strictly endogeic centipede *Clinopodes carinthiacus* (Latzel, 1880) is currently considered a single species inhabiting the south-eastern Alps, the northern Dinarides and, possibly, also other parts of the Balkan Peninsula (Bonato *et al.*, 2011), but the eastern range boundaries are still unknown. The south-eastern Alps show a remarkable environmental diversity, have a complex biogeographical history and are known to harbour a large amount of soil animal biodiversity, in terms of both species richness (also for centipedes; Peretti & Bonato, 2018) and the differentiation of intraspecific lineages (e.g. Stefani *et al.*, 2012; Bonato *et al.*, 2018; Štundlová *et al.*, 2019). Thus, this region stands out as a good study area for investigating species boundaries in population systems of small endogeic animals.

After searching populations of *C. carinthiacus* across the south-eastern Alps, we investigated species boundaries on the sampled specimens through an integrative approach. In detail, we analysed molecular and morphological variation independently and applied different methods of species discovery and delimitation without any a priori assumption regarding the number of species. As a preliminary assessment, we investigated individual morphological variation in selected populations, in order to discriminate interpopulation differences from variation deriving from ontogenetic allometry and sexual dimorphism. Finally, we identified the most likely hypothesis of species delimitation according to a criterion of congruence between alternative hypotheses obtained from different sources and methods. Based on these results, we also investigated differences in molecular sequences, morphological characters, geographical distribution and climatic niche between the resulting species and explored intraspecific between-population variation in more detail.

MATERIAL AND METHODS

STUDY AREA

The study area (Fig. 1) included the south-eastern Alps, as defined by the SOIUSA geographical classification (Marazzi, 2005), and the northern part of the Dinarides and contiguous reliefs eastwards to 15.7°E and southwards to 45.5°N, for a total extent of ~55 300 km².

FIELD SEARCHING AND SAMPLING

We visited 55 sites across the study area. Sites were chosen in consideration of the few published records of *C. carinthiacus* under its current taxonomic delimitation (Bonato *et al.*, 2011) and the presumed habitat of the species (i.e. broadleaf and mixed forests, with developed soil, at 600–1500 m a.s.l.). To
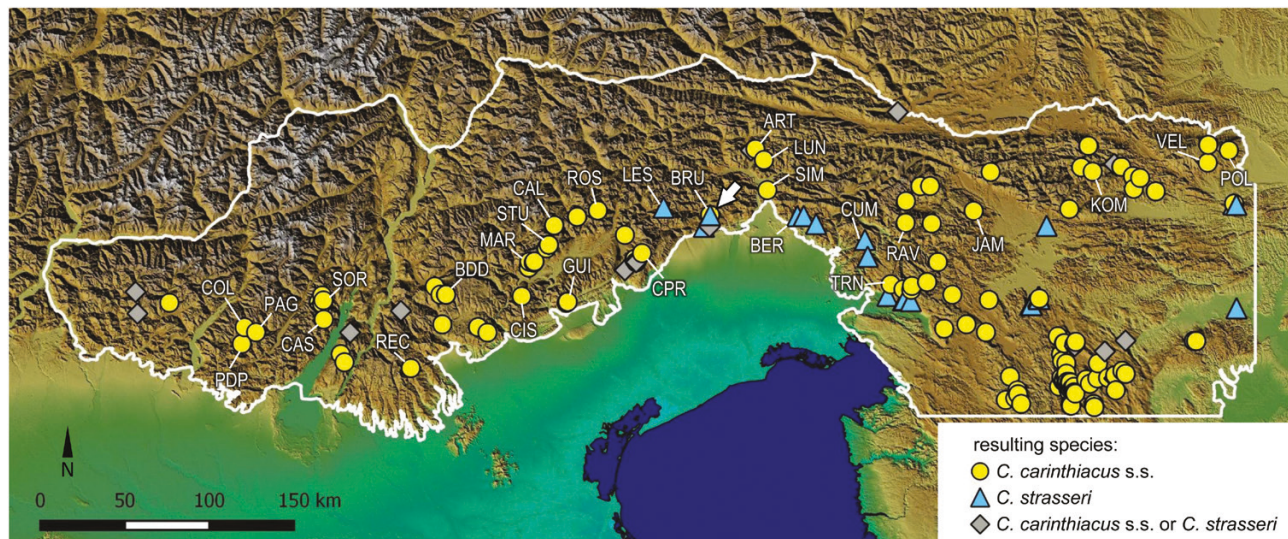
Figure 1. Study area (white contour), sampling sites for the integrative species delimitation analysis (labelled symbols; codes as in Table 1) and all other sites of occurrence based on confidently identified specimens and validated published records (symbols without labels). Sites of occurrence of the two resulting species are distinguished (see key), and the single site of syntopy is indicated (white arrow).

avoid effects of human-mediated translocations, we considered only sites that had remained covered by forest in the last two centuries and were not disturbed by human activities other than wood harvesting. For each site, all geophilomorph centipedes were collected within an area < 1 ha (hm²), entirely covered by tree canopy, uniform in major features of the ground and ≥ 10 m away from forest edges, roads or other human artefacts. Each site was visited between one and four times on different days in the years 2016–2019. During each visit, centipedes were searched for by hand in the soil and under stones, pieces of bark and other shelters, by between one and five people working simultaneously for ≥ 1 h.

IDENTIFICATION AND SELECTION OF SPECIMENS

Specimens of *C. carinthiacus* were identified in the laboratory, according to the current diagnosis of the species (Bonato *et al.*, 2011, 2014). We used both a stereoscopic microscope (Leica MZ12.5) and a light microscope (Leica DMLB) after mounting each specimen on a temporary slide with ethane-1,2-diol. Sex was assessed by examination of the gonopods.

We found 66 specimens of the target species, 10–33 mm long, from 27 of the 55 sites (Fig. 1; Table 1; Supporting Information, Tables S1 and S2). These sites were ≥ 6 km apart from the nearest site and separated by areas with habitats unsuitable for *Clinopodes* C. Koch, 1847 species (large rivers or areas deforested for centuries).

For each specimen, after measurement of length and counting the legs, the middle portion of the body was used for DNA extraction and the remaining anterior and posterior parts underwent morphological examination.

SPECIES DELIMITATION BASED ON GENETIC DIFFERENTIATION

DNA extraction, amplification and sequencing

DNA was extracted with the DNeasy Blood and Tissue kit (Qiagen, Hilden, Germany) according to the manufacturer's protocol. We amplified three genes that have been used successfully for other molecular studies in Chilopoda (e.g. Murienne *et al.*, 2010), also in the framework of integrative taxonomy (Joshi & Edgecombe, 2018; Joshi *et al.*, 2020): the mitochondrial 16S rRNA with the primer pair 16Sa/16Sb (Edgecombe *et al.*, 2006), the mitochondrial cytochrome *c* oxidase subunit I (*COI*) with the primer pair LCO1490/HCO2198 (Folmer *et al.*, 1994) and a fragment of the nuclear 28S rRNA with the new primer pair 28SIClinoFor (AGTCGTAGGGTCTGC TTCC)/28SIClinoRev (ATGTCCGTGCTTCAATCC). Polymerase chain reactions (PCRs) were performed in 20 µL reaction volumes containing 4.0 µL of 5× Flexi Buffer, 0.4 µL of 10 mM dNTPs, 0.8–1.0 µL of 25 mM MgCl$_2$, 0.5 µL of 100% dimethyl sulfoxide, 1.0 µL of each 10 µM primer, 0.1 µL of 5 U/µL GoTaq Flexi DNA Polymerase (Promega, Madison, WI, USA), 1 µL of template DNA and purified water. The reaction was carried out as follows: 5 min at 95 °C; 25–38 cycles of

Table 1. Sampling sites and number of specimens used for different analyses

Site			Number of specimens					
				Species delimitation				
Mountain range	Code	Name	Preliminary analysis of within-population morphological variation	16S	COI	28S	Morphology	Subsequent analysis of between-population morphological differences
Brescia Prealps	PDP	Mount Ario: W slope: Passo delle Piazze	–	1	1	1	1	5
	COL	Mount Colombine: Valle Serramando: Ronco	–	3	2	2	3	5
	PAG	Corno Barzo: N slope: Paghera	–	2	1	1	2	5
Garda Prealps	SOR	Val di Concei: Val Sorda	–	2	1	2	2	–
	CAS	Val di Ledro: Val Casalino	–	2	3	3	2	–
Western Venetian Prealps	REC	Piccole Dolomiti: Recoaro Mille	–	1	1	1	1	–
	BDD	Altopiano dei Sette Comuni: Bosco del Dosso	–	4	4	4	4	–
Eastern Venetian Prealps	CIS	Mount Grappa: Mount Cismon: NE slope	–	2	2	2	2	–
	GUI	Mount Cesen: Val Caldanè, near Guia	–	5	4	3	5	5
	CPR	Cansiglio: Pian Rosada-Pich	–	2	3	2	2	–
Southern Dolomites	MAR	Val di Lamen: Maragno	17	4	4	4	3	5
	STU	Val Canzoi: Lago della Stua	–	1	1	1	1	–
	CAL	Val del Mis: California	–	3	3	3	3	5
	ROS	Val del Grisol: Ponte dei Ross	–	3	2	3	2	5
Carnic Prealps	LES	Val Cellina: Bosco Lesis	–	1	0	0	1	–
	BRU	Mount Valinis: Brusat	13	6	7	6	7	–
	ART	Rio Radina valley, near Arta Terme	–	1	0	0	1	–
	LUN	Mount Sernio: Lunze	–	1	0	0	1	–
	SIM	Mount San Simeone: Casera San Simeone	18	3	2	3	3	5
Julian Prealps	BER	La Bernadia: Mount Lédina: E slope	–	1	1	2	1	–
	CUM	Mount Cum: NW slope	–	2	3	3	3	–
Trnovski gozd	TRN	Trnovo: Nemci	–	1	2	2	2	–
Julian Alps	RAV	Rodica: Kneža valley: Kneške Ravne	–	0	2	1	2	–
Western Slovene Prealps	JAM	Jelovica: Jamnik	–	1	1	1	1	–
Kamnik–Savinja Alps	KOM	Komen: Bezovec	–	2	2	2	2	–
North-eastern Slovene Prealps	VEL	Veliki vrh: Kos	–	2	2	1	2	–
	POL	Mala Polskava: Lobanškov kogel	–	2	2	1	2	–

Sites are arranged approximately from west to east (Fig. 1). Mountain ranges refer to the SOIUSA classification of the Alps (Marazzi, 2005). Coordinates and elevations are given in the Supporting Information (Table S1).

1 min at 94 °C + 1 min at 40–59 °C + 1.5 min at 72 °C; and 7 min at 72 °C. The PCR products were purified using a MinElute PCR purification kit (Qiagen) and sequenced on both strands with the same primer pairs as used for amplification. Sanger sequencing was performed either by Eurofins MWG Operon (Munich, Germany) or by BMR Genomics (Padova, Italy). Chromatograms were checked visually for signal intensity and quality using FINCH TV 1.4.0 (Geospiza, PerkinElmer). The sequence data have been submitted to the GenBank database under accession numbers MZ425120–MZ425176 and MZ427346–MZ427458.

Sequence alignment

Sequences were aligned with MAFFT (Katoh & Standley, 2013), with the L-INS-i algorithm for *COI* and the Q-INS-i algorithm for 16S and 28S, setting default parameters. To remove ambiguously aligned regions, the 16S and 28S alignments were subsampled using GBLOCKS (Castresana, 2002), with low stringency options as implemented in SEAVIEW (Gouy *et al.*, 2010). Next, the 28S alignment was corrected manually for one base shift between identical sequences, whereas the 16S alignment underwent a further GBLOCKS subsampling with high stringency options because residual ambiguities could not be resolved manually. Terminal regions of different length were removed manually.

Sequence distances

Pairwise distances between sequences were calculated as p-distances for 16S and 28S, whereas for *COI* they were corrected by the Kimura two-parameter (K2P) model, which accounts for multiple mutational hits, because *COI* alignment showed substitution saturation. Distances were calculated with MEGA (Kumar *et al.*, 2016). Indels were treated with pairwise deletion. Haplotype networks were obtained with POPART (Leigh & Bryant, 2015) by median joining (16S and 28S) or TCS (*COI*).

Sequence-based species delimitation methods

We used four methods for species discovery and delimitation from sequence variation: automatic barcode gap discovery (ABGD; Puillandre *et al.*, 2012); assemble species by automatic partitioning (ASAP; Puillandre *et al.*, 2021); general mixed Yule coalescent (GMYC; Pons *et al.*, 2006); and the Poisson tree process (PTP; Zhang *et al.*, 2013). ABGD clusters sequences into candidate species, based on their pairwise distances, by detecting an expected difference between (lower) values of intraspecific distances and (higher) values of interspecific distances (i.e. a 'barcoding gap').

ASAP clusters sequences into candidate species based on their pairwise distances like ABGD but ranks the alternative hypotheses of species delimitation considering both the probability of panmixia under the coalescent model and the barcode gap. Both GMYC and PTP are tree-based methods using coalescent theory to discern within-population and between-species processes. In an ultrametric tree (i.e. with branch length proportional to absolute or relative time), GMYC estimates an expected change of the branching rate along the tree between the branching attributable to speciation events (described by the Yule model) and the branching attributable to within-population substitutions (coalescent model). A confidence interval is estimated for the total number of candidate species. PTP is similar to GMYC, but does not require an ultrametric tree and can estimate Bayesian posterior probabilities for the candidate species.

Implementation of ABGD and ASAP

We ran ABGD considering 1000 steps in a range of prior values of maximum intraspecific distance (P) of 0.001–0.12 for 16S, 0.001–0.21 for *COI* and 0.001–0.07 for 28S. Upper values of P were selected in order to cover most of the range of variation of the distances calculated for each gene. We specified no prior minimum relative gap width (*X*). We ran ASAP considering a threshold value of probability of 0.01 to split a group of sequences into different candidate species.

Implementation of GMYC and PTP

Both methods were applied to the two mitochondrial DNA genes (16S and *COI*) separately, whereas they were not applied to 28S because for this gene we obtained a low number of poorly variable haplotypes. One of the methods (PTP; see below) was also applied to a concatenation of the three genes, although the signal of one gene could swamp the signal of the others (Fontaneto *et al.*, 2015).

To build gene trees, we produced alignments using MAFFT (see above), using sequences of the closely related species *Clinopodes flavidus* C. L. Koch, 1847 as an outgroup. The 16S sequence of the outgroup was obtained anew from a specimen from the southern Dolomites (GenBank accession number MZ427910), whereas for *COI* and 28S we used already available sequences (JN306671.1 and EU376008.1, respectively).

For the single genes, we used JMODELTEST (Posada, 2008) to find the best-fitting substitution models, following both the corrected Akaike information criterion (cAIC) and the Bayesian information criterion (BIC). PHYML (Guindon *et al.*, 2010) was used to produce two maximum likelihood (ML) trees

per gene by averaging the models selected by means of the cAIC and BIC, respectively. For our purposes, we used the cAIC-model-averaged tree for 16S, because of the higher bootstrap node supports, and the BIC-model-averaged tree for *COI*, because this, at variance with the cAIC-model-averaged tree, contained no polytomies.

For the concatenated dataset, IQ-TREE (Nguyen *et al.*, 2015; Trifinopoulos *et al.*, 2016) was used to produce a ML tree phylogeny. The best-fitting model for each partition (each corresponding to one gene) was estimated by MODELFINDER (Kalyaanamoorthy *et al.*, 2017) according to the cAIC, as implemented in IQ-TREE.

Ultrametric trees were obtained for each gene using RELTIME (Tamura *et al.*, 2012) in MEGA, which uses a relative time calibration. For the calibration, we used the best-fitting substitution models according to cAIC for 16S (TrN+I+G) and the best-fitting model according to BIC for *COI* (HKY+I+G). The procedure was not applied to the concatenated dataset, because the RELTIME algorithm does not manage different substitution models for different partitions. Accordingly, GMYC, which requires an ultrametric tree, was not applied to the concatenated dataset.

The outgroups were removed from the trees before running the GMYC and PTP. We used GMYC in both its single threshold (ST-GMYC) and multiple threshold (MT-GMYC; Monaghan *et al.*, 2009) implementations and PTP in both the original ML and the Bayesian (bPTP) implementation.

SPECIES DELIMITATION BASED ON MORPHOLOGICAL DIFFERENTIATION

Preliminary analysis of within-population morphological variation

We performed a preliminary assessment of the within-population variation of a first set of 23 characters (Supporting Information, Table S3) to select suitable characters for the species delimitation analysis. We considered all putative discriminating characters so far reported between species or infraspecific nominal taxa in the genus *Clinopodes* (Bonato *et al.*, 2011; Bonato & Minelli, 2014). Of all these characters, one is binary, two are meristic and the others are continuous, deriving from distance measurements (Supporting Information, Table S4; Fig. S1) taken with an ocular micrometre of the DMLB microscope. We evaluated whether and how each character varied in relation to body size and sex in each of the three sites where we collected the largest numbers of specimens (13–18 specimens for each site; Table 1), assuming all specimens from a single site to be conspecific. The width of the forcipular coxosternite was used as an index of body size. Data were collected by a single person (L.B.) to control for observer bias.

A linear mixed model was built for each character, with body size and sex as fixed factors, including their interaction. The site was treated as a random factor because this preliminary analysis was intended to evaluate the effects of body size and sex and not to estimate differences between populations and/or species. Generalized linear mixed models were built for the meristic characters, assuming a Poisson distribution and a logarithmic link function. The statistical significance of the effects of body size, sex and their interaction was assessed through the Wald test. The analyses were carried out with the R package lme4 (Bates *et al.*, 2015).

Model-based cluster analysis

For the species delimitation analysis, ten quantitative characters were selected among all those evaluated previously for within-population variability (Table 2) and measured on 61 specimens sampled from the 27 sites (Table 1; Supporting Information, Table S2). We included all characters showing no significant variation associated with either body size or sex and those showing substantial among-population differences, after simple transformations (e.g. into proportion measurements) were applied to minimize the effects of body size or sex. Specifically, for the number of leg pairs, we added two pairs to the number counted in males because we found an average difference of two pairs between sexes in each population (see Results below), as is common in many other geophilids (reviewed by Minelli & Koch, 2011). For this dataset, the ten characters were measured anew by a single person (E.P.) to control for observer bias.

To delimit a set of candidate species, we performed a model-based cluster analysis of the specimens based on the overall variation of the ten selected characters, which were standardized to have a mean of zero and standard deviation of one. Multiple 'normal mixture models' differing in the number of candidate species were fitted to the multivariate dataset, estimating the parameters with the Expectation Maximization algorithm, and the best model was selected according to the BIC (Fraley & Raftery, 2002; Bouveyron & Brunet-Saumard, 2014). The analysis was carried out with R package mclust 5.0 (Scrucca *et al.*, 2016).

EVALUATION OF SPECIES DELIMITATION HYPOTHESES

Given that different sources of evidence and different analytical methods produced dissimilar hypotheses of species delimitation, differing in either the number of candidate species and/or the partition of the specimens into the candidate species, the hypothesis

Table 2. Morphological characters used in the species delimitation analysis and differences between the two resulting species

| Character | | *Clinopodes carinthiacus* s.s. (N = 52) | *Clinopodes strasseri* (N = 9) | Test for difference | | Discriminant analysis (with/without transformation) | |
Name	Definition	(mean ± SD)	(mean ± SD)	t or W	P-value	Coefficient	P-value
Distal elongation of antennae	Ratio between length and width of article XIV of antennae	1.96 ± 0.09	2.02 ± 0.11	t = −1.39	0.195	0.00/0.04	1/1
Relative breadth of forcipular coxosternite	Ratio between width and length of forcipular coxosternite	1.40 ± 0.06	1.35 ± 0.05	t = 2.67	0.019	−0.08/−0.23	1/1
Elongation of denticles*	Ratio between maximum length of the coxosternal denticles and width of head	0.022 ± 0.004	0.058 ± 0.08	W = 0.0	0.000	2.41/0.10	0.000/1
Number of setae on sternite 1	Number of setae and all other projecting sensilla on the metasternite of leg-bearing segment 1	15 ± 4	15 ± 2	t = 0.41	0.685	−0.16/−0.55	1/1
Number of setae on sternite 2	Number of setae and all other projecting sensilla on the metasternite of leg-bearing segment 2	28 ± 6	31 ± 9	t = −0.96	0.362	0.43/0.71	1/1
Corrected number of pairs of legs*	Number of leg pairs + 2 if the specimen is male	56 ± 1	61 ± 1	W = 0.5	0.000	1.12/2.03	0.664/0.002
Relative breadth of penultimate sternite	Ratio between width and length of metasternite of the penultimate leg-bearing segment	0.88 ± 0.07	0.84 ± 0.08	t = 1.46	0.175	−0.02/0.03	1/1
Elongation of ultimate pore-field	Ratio between length of pore-field and length of metasternite of penultimate leg-bearing segment	0.57 ± 0.06	0.53 ± 0.16	t = 0.82	0.434	−0.12/0.09	1/1
Degree of posterior narrowing*	Ratio between width of ultimate sternite and width of forcipular coxosternite	0.37 ± 0.03	0.38 ± 0.03	W = 198.5	0.470	0.02/0.29	1/1
Relative number of coxal pores*	Ratio between average number of coxal pores on each coxopleuron and length of the coxopleuron	30 ± 5	30 ± 4	W = 212.5	0.662	0.26/−0.11	1/1

The terminology of anatomical parts follows Bonato *et al.* (2010). Differences were tested with either Welch's *t*-test (*t*) or Wilcoxon's test (*W*), depending on the statistical distribution of the data (Supporting Information, Table S13).
*The stepwise discriminant analysis was repeated after the transformation ($-1/x$) of the non-normal characters indicated with an asterisk.

most frequently retrieved (i.e. consistently indicated by the broadest array of sources and methods) was considered as the best supported (e.g. see Padial *et al.*, 2010; Carstens *et al.*, 2013).

Differences between the resulting species

Morphology

The relative contribution of the ten morphological characters (Table 2) in separating the resulting species was assessed through a stepwise discriminant analysis (canonical variate analysis) performed in R with the package multiDimBio (Scarpino, 2020). The analysis was carried out twice: firstly, on the original variables (standardized to have a mean of zero and standard deviation of one) and secondly, after the appropriate transformation to conform to a normal distribution (Table 2).

Geographical distribution

Specimens collected from many other sites within the study area (Fig. 1) and preserved in our collections (Bonato–Minelli collection, University of Padova; Kos collection, University of Ljubljana) were re-examined and assigned to the resulting species based on the morphological characters that were found to be diagnostic with the discriminant analysis (see above).

We also digitized all published records that had been assigned to *C. carinthiacus* or synonyms. Published records were excluded when either erroneous or uncertain in one of the following cases: (1) published morphological data for the voucher specimen(s) were inconsistent with the morphology of the species complex under study; (2) doubts on the species identity were expressed by the author(s); and (3) the locality was clearly isolated from all other reliable records, and the author(s) did not indicate criteria, sources and characters for the identification. Reliable published records were assigned to one of the resulting species only when diagnostic morphological characters were reported.

Most records were georeferenced originally, with precision to the nearest 10 m and coordinates rounded at the fourth decimal digit in decimal degree notation. For the remaining records, the position was estimated with variable precision, between 0.1 and 10 km, and the coordinates were rounded at the third, second or first decimal digit accordingly.

Climatic niche

To test for differentiation in the realized climatic niche between the resulting species, we considered three major climatic parameters (minimum temperature, seasonal variation of temperature and rainfall) in the entire study area (Fig. 1). These parameters are expected to affect the occurrence of soil-dwelling animals, as indicated by empirical studies of species distribution modelling, also for centipedes (Georgopoulou *et al.*, 2016).

In detail, we considered the following three bioclimatic variables from WorldClim (Hijmans *et al.*, 2005): minimum temperature of the coldest month (BIO6); annual variance of temperature (BIO4); and annual precipitation (BIO12). These variables were selected among the least correlated between each other within our study area (pairwise Pearson's r = 0.0–0.3; Supporting Information, Table S5). Variables BIO3, BIO14 and BIO15 were not considered, following Bedia *et al.* (2013) and Varela *et al.* (2015). Bioclimatic data were retrieved with a resolution of 30″ (~1 km in the study area).

We considered only records with geolocalization error ≤ 1 km and confidently assigned to one of the resulting species (see above). In order to minimize site autocorrelation, records of each resulting species were filtered to eliminate site duplicates and, whenever two records were closer than 1 km, only one of the two was chosen randomly for the analysis.

Niche differentiation was tested for any pair of species, following Broennimann *et al.* (2012) and by modelling the realized niche of the species as an *n*-dimensional hypervolume. The method of Broennimann *et al.* (2012) was applied with the R package ecospat (Di Cola *et al.*, 2017). A principal components analysis was carried out on the values of the selected bioclimatic variables in the entire study area. The distribution of each species along the principal components was smoothed by a kernel density function. Schoener's D index of niche overlap between two species (from zero = no overlap to one = complete overlap) was calculated based on the occupancy values after correction for the variation of the principal components in the study area. To test whether D was significantly lower than expected by chance, we performed a 'niche equivalency' test (Warren *et al.*, 2008; Broennimann *et al.*, 2012), setting the argument 'alternative' = 'lower' (see Di Cola *et al.*, 2017). The observed value of D was compared with the frequency distribution of D estimated from random samples of sites extracted from the pooled set of sites of the two species, maintaining the original sample sizes, for 1000 randomization rounds. To control for the possible effect of records with poor georeferencing, we repeated the analysis considering only records with geolocalization error ≤ 10 m.

The hypervolume analysis was carried out with the R packages hypervolume (Blonder, 2018) and BAT (Cardoso *et al.*, 2021). The values of the selected bioclimatic variables in the sites were extracted, and a principal components analysis was carried out after scaling the variables to have a mean of

zero and standard deviation of one. Hypervolumes were calculated through Gaussian kernel density estimation, with the bandwidth estimated with cross-validation. The relevant metrics (hypervolume volume and shared volume) and indices of hypervolume similarity (Jaccard and Sørensen–Dice indices) were calculated with BAT.

INTRASPECIFIC MORPHOLOGICAL VARIATION

To assess the morphological variation between populations within a single species, we considered the most widespread of the resulting species and selected five specimens assigned confidently to that species from each of the eight sites with sufficiently large samples (Table 1). We considered only specimens with body length ≥ 15 mm to minimize the expected variation in shape associated with growth (ontogenetic allometry) and only females to control for sexual dimorphism.

We considered the same distance measurements used previously in the analysis of within-population variation (see above), for a total of 23 measurements (Supporting Information, Table S4). All measurements were collected by a single person (C.C.) to control for observer bias. Specimens were examined in randomized order, and measurements were taken twice, after removal and replacement of the specimens on the microscope slide.

Between-population differences were tested by means of a MANOVA after averaging replicates within specimens. Variables were checked for normality with the Shapiro–Wilk test and standardized to have a mean of zero and standard deviation of one. Whenever necessary (two distance measurements), data were transformed to conform to the assumption of normality. Additionally, between-population differences in the number of legs were evaluated by means of Kruskal–Wallis ANOVA. Analyses were carried out in R.

We also analysed the shape of the forcipular coxosternite, which features as a major functional apparatus involved in prey catching and feeding, by means of geometric morphometrics (Bookstein, 1991). Following Baiocco *et al.* (2017), we considered 11 landmarks and six semilandmarks (Supporting Information, Table S6), which were chosen approximately coplanar in order to mitigate the error stemming from the projection of the three-dimensional structure (Cardini, 2014). Images of the forcipular coxosternite in ventral view were obtained at a standardized magnification by using a digital camera (Leica DFC 400) mounted on the light microscope. Image stacks with different focal planes were integrated with COMBINE ZP (Hadley, 2008). Each image was obtained twice, after removal and repositioning of the specimen on the microscope slide,

and for each image all landmarks and semilandmarks were digitized twice, on different days, processing specimens in a randomized order. Landmarks and semilandmarks were digitized with TPS-DIG2 (v.2.31; Rohlf, 2015). Image acquisition and landmark and semilandmark digitization were carried out by a single person (C.C.) to control for observer bias. Semilandmark coordinates were allowed to slide along the profile to minimize bending energy in TPSRELW32 (v.2.69; Rohlf, 2015). The generalized Procrustes superimposition algorithm was used to remove differences in size, position and orientation between landmark configurations, transforming raw coordinates into shape coordinates (Rohlf & Slice, 1990). Given that the forcipular coxosternite has bilateral symmetry ('object symmetry'), the variation in shape was partitioned into its symmetric and asymmetric components, and differences between populations were investigated by concentrating on the symmetric component (Klingenberg *et al.*, 2002). Between-population differences were tested by Procrustes ANOVA and evaluated by between-group principal components analysis (Mitteroecker & Bookstein, 2011), after averaging replicas within specimens. These analyses were carried out with MORPHOJ v.1.06c (Klingenberg, 2011) and PAST v.3.18 (Hammer *et al.*, 2001).

RESULTS

SPECIES DELIMITATION BASED ON GENETIC DIFFERENTIATION

Molecular variation

We obtained multiple alignments of 421 bp for 16S, 608 bp for *COI* and 686 bp for 28S. Among the mitochondrial genes, 16S was less variable than *COI* (16 haplotypes with a maximum pairwise distance of 11.6% vs. 25 haplotypes with a maximum pairwise distance of 25.7%, respectively), whereas the nuclear 28S was even less variable (nine haplotypes with a maximum pairwise distance of 7.2%). Only one specimen was found to be heterozygous for 28S, but its two alleles collapsed in a single haplotype after alignment trimming.

The haplotype networks (Supporting Information, Fig. S2) indicated many highly divergent groups for both 16S and *COI*, but only two highly divergent groups for 28S. Considering the geographical distribution of the groups of similar haplotypes (Supporting Information, Fig. S2), both 16S and *COI* showed two or three groups with contiguous distributions in the western and intermediate part of the study area (between the Brescia Prealps and the eastern Venetian Prealps) and other single divergent haplotypes in the easternmost

part of the study area (between the Carnic Prealps and the north-eastern Slovene Prealps). Conversely, 28S showed a single group in most sites of the study area. Additionally, for all three genes, some sites in the Carnic and the Julian Prealps showed a single group of similar haplotypes, highly divergent from the others. It is noteworthy that different specimens from a single site in the Carnic Prealps (BRU in Fig. 1) showed two deeply diverging haplotypes for all genes (with distances of 11.2% for 16S, 23.7% for *COI* and 6.4% for 28S).

ABGD and ASAP analyses

For 16S, the ABGD analysis indicated a single species for a maximum intraspecific distance (P) > 2.9%, and alternative hypotheses of partition into two, four, three and nine candidate species for lower and lower values of P (Supporting Information, Fig. S3), with the best score assigned by ASAP to the nine-species hypothesis (Fig. 2). For *COI*, the ABGD indicated a single species for P > 8.0%, then two, three, seven and more candidate species for lower values of P (Supporting Information, Fig. S3), with the best score assigned by ASAP to a hypothesis of 13 species (Fig. 2). For 28S, the ABGD indicated a single species for P < 6.4% and two stable hypotheses of three or two candidate species for higher values of P (Supporting Information, Fig. S3); both hypotheses received the best score by ASAP (Fig. 2).

Only the hypothesis of two species was recovered consistently for all three loci, also in terms of specimen composition: one candidate species was spread across the investigated area, whereas the other species inhabited only a small area between the Carnic and the Julian Prealps. It is noteworthy that the different specimens with highly divergent haplotypes from the site BRU in the Carnic Prealps were assigned to one or the other of these two candidate species. Other hypotheses of higher numbers of species were incongruent in the composition of specimens between the three loci.

GMYC and PTP analyses

After including the outgroup, the multiple alignment became 416 bp long for 16S, 608 bp long for *COI* and 659 bp long for 28S. We obtained an ML tree of the 16 ingroup haplotypes of 16S, with all nodes supported by 81–100% bootstrap values, and an ML tree of the 25 ingroup haplotypes of *COI*, with all nodes supported by 71–100% bootstrap values (Fig. 2). A total of 14 candidate species (confidence interval: eight to 14) were indicated by the ST-GMYC analysis of 16S, and nine species (confidence interval: eight to nine) by the MT-GMYC analysis (Fig. 2). Instead, ≤ 18 species (confidence interval: 17–18) were indicated by the
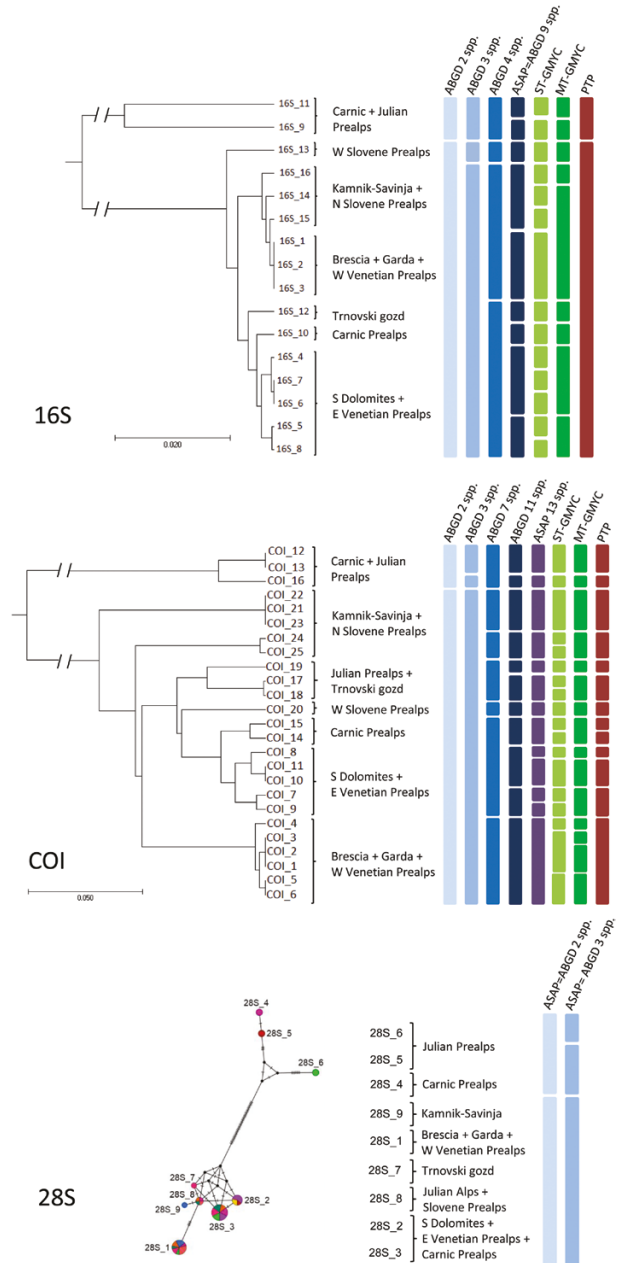

Figure 2. Subdivision of 16S, *COI* and 28S haplotypes into candidate species according to different species delimitation methods. The ultrametric trees used for the general mixed Yule coalescent (GMYC) analyses are illustrated for the haplotypes of 16S and *COI* (all nodes: bootstrap supports ≥ 81% for 16S and ≥ 71% for *COI*). The median-joining network is illustrated for the 28S haplotypes (see also Supporting Information, Fig. S2). Mountain ranges where the haplotypes were found are also indicated.

ST-GMYC analysis of *COI* and 15 (confidence interval: 12–16) by the MT-GMYC (Fig. 2).

A much more lumped hypothesis of only two species resulted from the PTP analysis of 16S, with both ML and Bayesian implementations (Fig. 2). The specimen composition of these two candidate species matched exactly the two-species hypothesis suggested by ABGD (see above). The Bayesian posterior probabilities were 0.52 for the candidate species widespread in the study area and 0.93 for the eastern species. Instead, 13 candidate species resulted from the PTP analysis of *COI*, with both ML and Bayesian implementations, with Bayesian posterior probabilities for the species in the range 0.74–1.00 (Fig. 2), and 11 species from the PTP analysis of the concatenated genes (Supporting Information, Fig. S4).

SPECIES DELIMITATION BASED ON MORPHOLOGICAL DIFFERENTIATION

Within-population morphological variation

Linear mixed models built for the full set of 23 morphological characters in samples of putative conspecific specimens revealed that some characters were significantly associated with body size (Supporting Information, Table S7): the head and the anterior trunk sternites became relatively stouter with increasing size; the forcipular segment became broader than the head; the setae and the coxal pores increased their maximum size; and the ultimate legs became relatively more slender. Additionally, a few characters were significantly associated with sex (Supporting Information, Table S7): the forcipular denticles of the smaller specimens were slightly more elongate in males than in females; the forcipules were slightly stouter in males and slightly more slender in females; males had, on average, two fewer pairs of legs than females; the sternite between the ultimate legs was stouter in males than in females; and the ultimate legs were usually more slender in females and slightly swollen in males.

Model-based cluster analyses

Based on the results of the preliminary analysis of within-population morphological variation (see above), we selected ten characters, aptly transformed to account for body size and sex whenever necessary (see Material and Methods; Table 2). In the model-based cluster analysis through normal mixture models, the best model (with the highest BIC value) partitioned the specimens into two groups (Fig. 3). All specimens were assigned unambiguously to one or the other group, with probability ~1.0. The same optimal number of two groups was retrieved by most of the normal mixture models (i.e. all those with 'diagonal' and 'spherical' distributions

and also some models with 'ellipsoidal' distributions; Fig. 3). This partition matched exactly the two-species hypothesis suggested by some of the molecular-based partitions (Fig. 2). Specimens found together in the site BRU were assigned to different species.

CONSENSUS SPECIES DELIMITATION HYPOTHESIS

The best-supported consensus hypothesis was a partition of the sampled specimens in two species; this was the only hypothesis that was retrieved both from the morphological analysis and from some of the molecular analyses. A consistent partition of specimens between two species, with the same specimen composition, was retrieved by the ABGD analyses on all the three molecular loci, the PTP analysis of 16S and the model-based cluster analysis applied to morphological characters. In detail, 56 specimens from 24 sites distributed throughout the study area were assigned to a species that should keep the name *Clinopodes carinthiacus s.s.*, whereas the remaining ten specimens from four sites in the Carnic and the Julian Prealps were assigned to another species that should be called *Clinopodes strasseri* (Verhoeff, 1938) (Fig. 1; see Discussion below for notes on species names). At one site (BRU), we found the two species in syntopy.

All other delimitation hypotheses retrieved by different analyses were inconsistent with each other, either for the number of species or for the partition of the specimens among species. The traditional single-species hypothesis was contradicted by most delimitation analyses, with the exception of ABGD and only assuming high values of intraspecific sequence variation. The pairwise genetic distances between the two resulting species were 9.7–11.6% for 16S, 20.8–25.7% for *COI* and 6.3–7.2% for 28S.

DIFFERENCES BETWEEN SPECIES

Morphology

Of the ten morphological characters used in the species delimitation analysis (see above), the two resulting species were found to differ significantly in the elongation of the coxosternal denticles and in the number of pairs of legs, which were the most significant characters retrieved in stepwise discriminant analyses performed under different options of data transformation (Table 2). In particular, *C. carinthiacus s.s.* had less elongate denticles than *C. strasseri* (~2% of the width of the head vs. ~6%; Fig. 3) and fewer pairs of legs (in females: 53–59, with a modal value of 55, vs. 59–61, with a modal value of 61; Fig. 4).
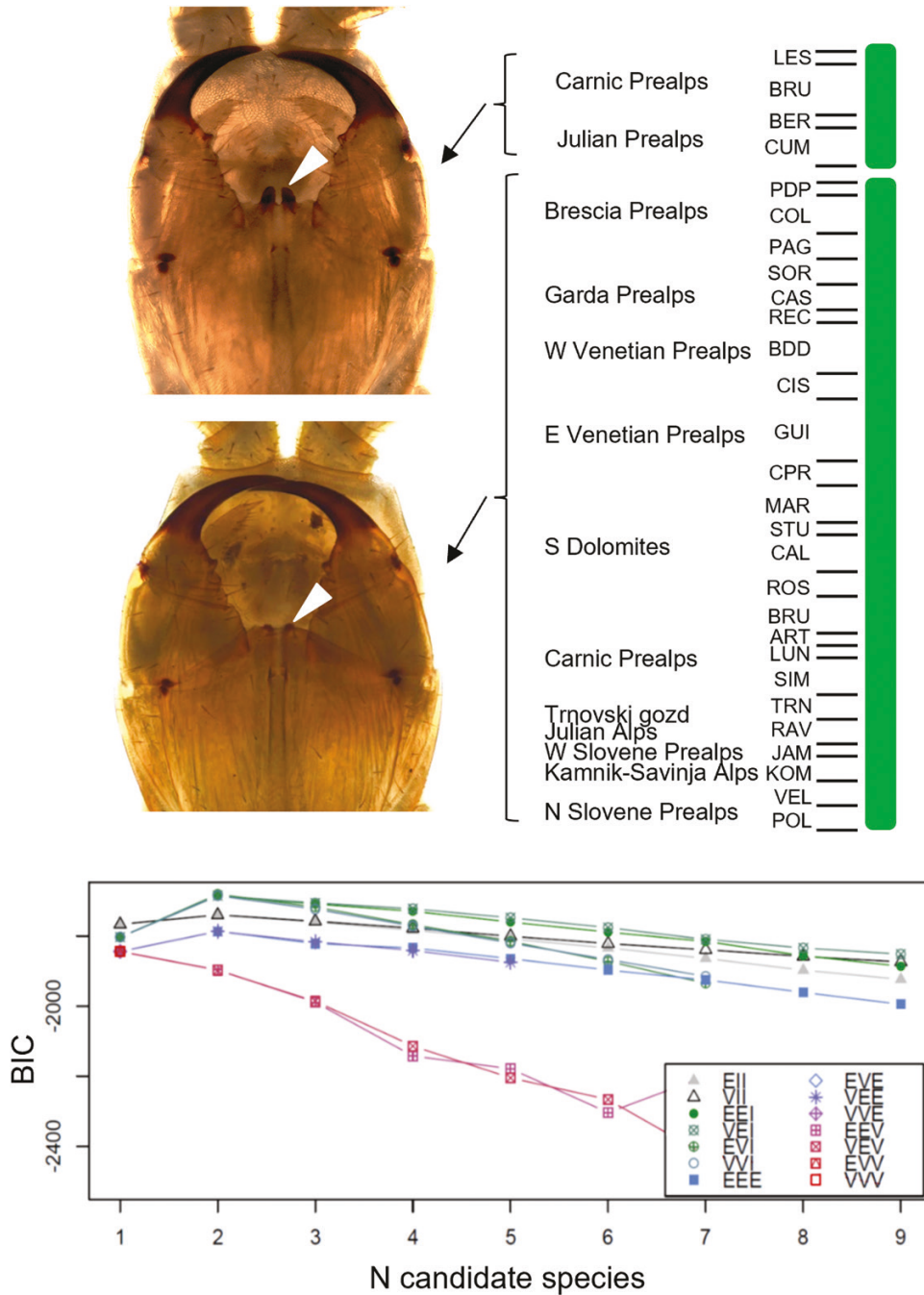
Figure 3. Subdivision of specimens into candidate species according to a model-based cluster analysis through normal mixture models on ten morphological characters (Table 2). The ventral view of the forcipular segment is illustrated for representative specimens of the candidate species. Denticles are indicated by arrowheads. The lower panel shows Bayesian information criterion (BIC) values of different models (coded as in the paper by Scrucca *et al.*, 2016) in relation to the hypothetical number of candidate species.

Geographical distribution

By evaluating the two most effective diagnostic characters (elongation of coxosternal denticles and number of legs; Table 2) in the other 1171 specimens collected from the study area, we confirmed that relatively elongated denticles are usually associated with higher numbers of legs (Fig. 4; Supporting Information, Table S8) and we could confidently identify 950 specimens from 132 sites as belonging to *C. carinthiacus s.s.* and 220 specimens from 20 sites as

belonging to *C. strasseri*. Moreover, after evaluating all published records, which are sparse in the scientific literature, we added reliable records of either species from another six sites.

As a result, *C. carinthiacus s.s.* was recorded from 136 sites throughout most of the study area, westwards to the Bergamasque Prealps (Orobian Prealps) and eastwards to the north-eastern Slovene Prealps (Pohorje), whereas *C. strasseri* was recorded from 23 sites, all in the eastern part of the study area, from the Carnic Prealps through the Julian Prealps to the Kamnik–Savinja Alps (Fig. 1). Besides the case of syntopy documented above (eight specimens of *C. carinthiacus s.s.* and 22 specimens of *C. strasseri* found together within 1 ha in Mount Valinis, Carnic Prealps; site BRU in Fig. 1), 12 specimens of *C. carinthiacus s.s.* were collected the same day only 0.1 km away from 16 specimens of *C. strasseri* near Draga pri Igu, northern Dinarides.
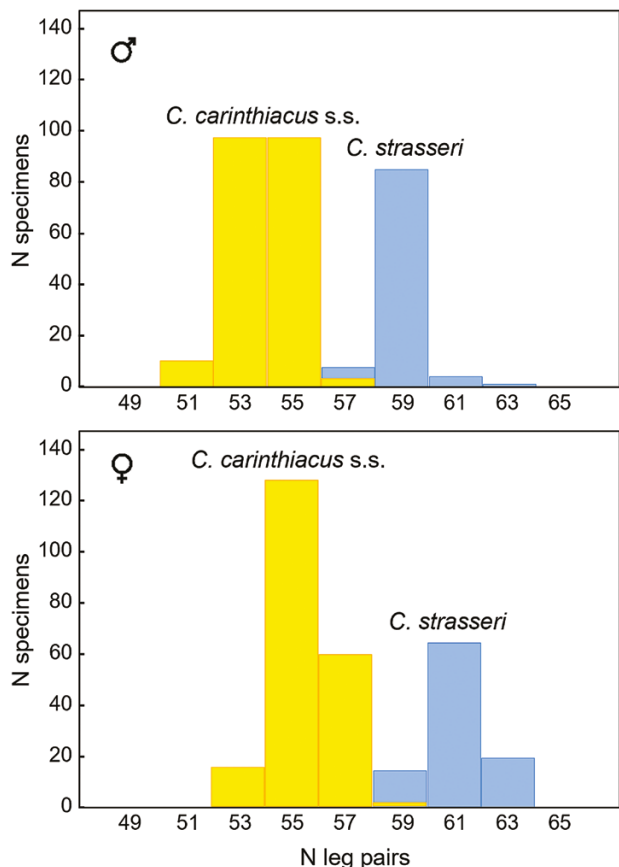

Figure 4. Number of pairs of legs in specimens confidently identified as belonging to *Clinopodes carinthiacus s.s.* and *Clinopodes strasseri* in the study area. Differences between species are statistically significant for both males and females (Mann–Whitney *U*-test: $P < 0.0001$ for both sexes; Supporting Information, Table S8).

Climatic niches

By applying the method of Broennimann *et al.* (2012), the first principal component of the selected bioclimatic variables in the study area (temperature minima, seasonal variation of temperature and rainfall) accounted for 48% of the total variation and was strongly correlated with lower temperature seasonality (Fig. 5) and, considering other correlated bioclimatic variables, with lower annual and circadian temperature variation (Supporting Information, Table S5). The second principal component accounted for another 32% of the total variation and described a gradient towards less abundant rainfall, both throughout the year and within single seasons, and less rigid winters and generally higher temperature over the year (Fig. 5; Supporting Information, Table S5).

Comparing the realized climatic niche of the two species (Fig. 5; Supporting Information, Fig. S5), Schoener's index of niche overlap ($D = 0.20$) was significantly lower than expected by chance under the null hypothesis of niche equivalency ($P = 0.007$; Supporting Information, Fig. S5A). The same result was obtained when considering only records with geolocalization error ≤ 10 m ($D = 0.21$, $P = 0.018$; Supporting Information, Fig. S5B). Although the two species inhabit a broad and largely similar range of climatic conditions, *C. carinthiacus s.s.* also inhabits sites with lower temperature seasonality, more rigid
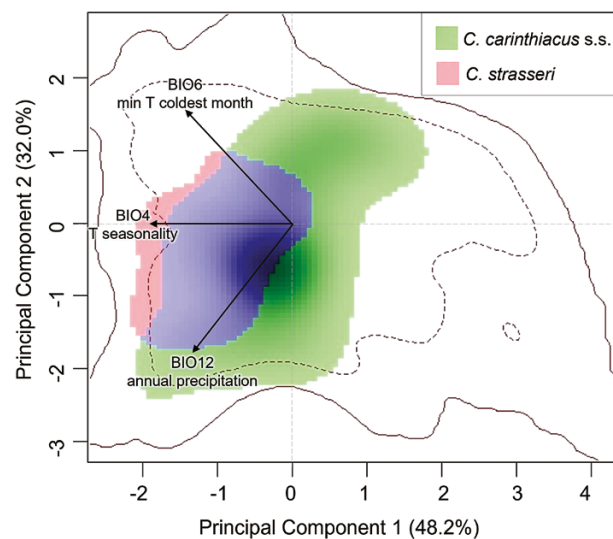

Figure 5. Contribution of the bioclimatic variables on the first two principal components of climatic variation in the study area, and density of occurrence of *Clinopodes carinthiacus s.s.* and *Clinopodes strasseri* on the two principal components estimated with ecospat, based on 106 sites (former species) and 16 sites (latter). Continuous and dashed contour lines indicate 100% and 50% of the available climatic space, respectively.

winters and both drier and wetter climates than *C. strasseri* (Fig. 5; Supporting Information, Table S9).

The realized climatic niches of the two species resulted in only partial overlap (Jaccard index = 0.28, Sørensen–Dice index = 0.44), as did the *n*-dimensional hypervolume analysis (shared volume = 40% of the *C. strasseri* hypervolume and 53% of the *C. carinthiacus* hypervolume; Supporting Information, Fig. S6). The hypervolume of the climatic niche of *C. strasseri* included sites characterized by a higher temperature seasonality, milder winter and higher annual rainfall. However, it was greater than the hypervolume of *C. carinthiacus s.s.* (volumes ~70 vs. 50), possibly because of the low number of occurrences of *C. strasseri* (16 sites), which could have led to an overestimation of the total volume because the method does not detect holes in the hypervolume (Blonder, 2016).

INTRASPECIFIC MORPHOLOGICAL VARIATION

By selecting females of comparable size (Kruskal–Wallis test on body size index: H = 11.2, P = 0.128) for eight populations of *C. carinthiacus s.s.* (Table 1), we found significant overall morphological variation between populations for the 23 distance measurements (MANOVA: Pillai's trace = 5.35, F = 1.55, d.f. = 161, P = 0.016; Supporting Information, Table S10). In particular, specimens from the COL, GUI and ROS populations differed markedly from those from the PDP and MAR populations, with a slightly larger size of the anterior trunk sternites and, with marginal significance, also of the forcipular structures. The COL and ROS populations also differed between each other in the sternite of the ultimate leg-bearing segment (shorter in the latter population).

The geometric morphometric analysis of the forcipular coxosternite showed statistically significant variation in shape between populations (Procrustes ANOVA: F = 2.43, P < 0.0001; Pillai's trace = 3.81, P < 0.0001; Supporting Information, Table S11), which accounted for 28.4% of the total variation in shape. The between-group principal components analysis performed on the shape coordinates showed that most of this variation affected the anterior margin of the coxosternite, where this articulated with the forcipules (between-group principal component 1, explaining 55% of the variance; Fig. 6), and secondarily, the general elongation of the coxosternite (between-group principal component 2, 20%; Fig. 6) and the extent of its lateral parts and denticles (between-group principal component 3, 14%; Supporting Information, Fig. S7). Also, the number of pairs of legs was significantly different between populations (Kruskal–Wallis ANOVA: H = 15.23, P = 0.033; median test: χ^2 = 14.34, P = 0.046), especially when comparing GUI (female

modal value 55) with CAL and ROS (female modal value 57) populations.

DISCUSSION

FIELD SAMPLING OF SMALL ENDOGEIC ANIMALS

The sample size in the present study (66 specimens) is smaller than desirable, but this is a common issue in species delimitation studies on small endogeic animals (e.g. Pérez-González *et al.*, 2018; Rota *et al.*, 2018). The collection of numerous fresh specimens of these animals is hindered by the following practical difficulties: (1) the geographical distribution of the target animals and the ecological drivers affecting their local distribution are often little known; (2) there are no effective methodologies to collect fresh specimens suitable for multiple analyses, including DNA extraction and sequencing, other than visual and hand search (e.g. Peretti & Bonato, 2018); and (3) populations of endogeic animals can occur at relatively low density, as is the case of predators, such as centipedes. As a result, sampling effort can be disproportionate with respect to the final sample size. For instance, in our study we employed > 320 person-hours, managing to detect target animals in about half of the visited sites, and most of the time, fewer than ten adult specimens per site were found in a day.

INTEGRATING EVIDENCE FOR SPECIES DELIMITATION

Considering genetic information (sequences of three molecular loci from both mitochondrial and nuclear genomes) and morphological information (ten characters encompassing different parts of the body), we obtained alternative hypotheses of species delimitation for the same set of sampled populations, depending both on the type of data (genetic vs. morphological) and on the method applied.

Despite on-going advances in handling data of different types (molecular sequences, morphometric data and geographical positions) in common Bayesian analyses (Eberle *et al.*, 2016; Hoban *et al.*, 2019), a standard and flexible methodology is still lacking for exploitation of the full diversity of sources of evidence. Consequently, alternative hypotheses of species delimitation derived from different sources and methods need to be compared *ex post*, but general principles and operational criteria are seldom declared explicitly. Following best practices in integrative taxonomic studies (e.g. Padial *et al.*, 2010; Carstens *et al.*, 2013), we took the most broadly and consistently retrieved hypothesis as the best supported. This sort of 'majority rule' (similar to that used in phylogenetic inference; Margush & McMorris, 1981; Dong *et al.*, 2010)
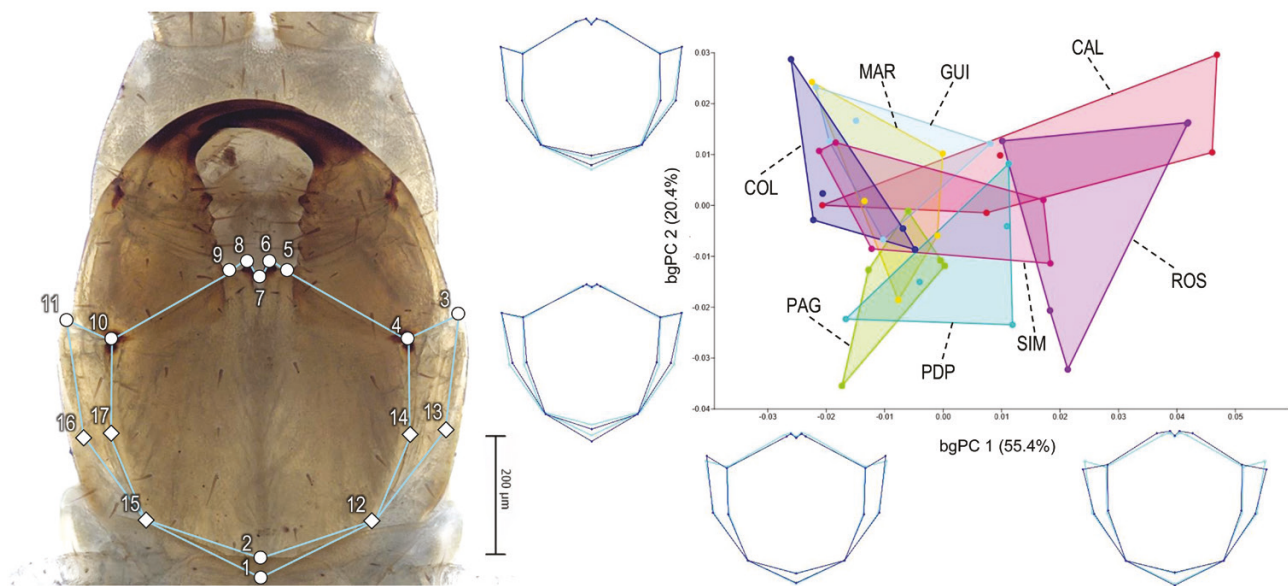
Figure 6. Geometric morphometric analysis of between-population variation of the shape of the forcipular coxosternite in *Clinopodes carinthiacus s.s.*. The left panel shows landmarks (circles) and semilandmarks (diamonds) on a representative specimen (PD-G 7787, from population GUI). The right panel shows the distribution of 40 specimens from eight populations (codes as in Table 1) on the first and second principal components (bgPC 1 and bgPC 2) obtained from a between-group principal components analysis of the symmetric component of the shape. Polygons indicate populations. The wireframes along the components represent the variation in shape (dark blue) in comparison to the average shape (light blue).

is grounded theoretically in the expectation that speciation produces a concordant pattern of divergence between multiple genetic and morphological traits over time. Conversely, it is assumed less likely that such a congruent pattern of divergence might emerge by chance within a single species (Padial *et al.*, 2010). This principle has been advocated repeatedly in species delimitation studies (e.g. Dayrat, 2005; DeSalle *et al.*, 2005; Padial *et al.*, 2010; Schlick-Steiner *et al.*, 2010). However, this was applied more frequently for corroborating a primary hypothesis of species delimitation than for choosing between competing hypotheses produced *de novo* by different data sources and analytical methods, as we did.

Although it has been possible to draw primary hypotheses of species delimitation from the molecular differentiation and the morphological differentiation evaluated through traditional morphometrics, we are still lacking adequate methodologies to draw primary hypotheses from other lines of evidence of speciation, such as ecological niche differentiation and subtle shape divergence, which could be captured by geometric morphometrics. Accordingly, we used climatic niche analyses only to corroborate a primary hypothesis of species delimitation, and we used geometric morphometrics to explore intraspecific variation between populations. New methodologies allowing us to make use of these approaches rigorously

in the 'species discovery' step, without any a priori hypothesis of species delimitation, would allow full exploitation of their potential in the framework of integrative taxonomy.

SPECIES DELIMITATION IN *C. CARINTHIACUS* IN THE SOUTH-EASTERN ALPS

In our case study, contrary to the traditional taxonomic opinion of a single species distributed across the south-eastern Alps and the northern Dinarides, a two-species hypothesis was retrieved from evidence of both molecular and morphological divergence. Species delimitation methods applied to mitochondrial loci suggested the existence of further differentiation between populations and therefore of other, less obvious species boundaries. With the exception of PTP applied to 16S, tree-based methods were prone to oversplit the datasets of 16S and *COI* sequences into a high number of candidate species. However, the GMYC method is known often to oversplit, especially when compared to the PTP, and this has usually been explained with errors in time calibration of the tree (Pentinsaari *et al.*, 2017). Unfortunately, the RELTIME method we used for time calibration was not included in the comparative analysis by Talavera *et al.* (2013), who tested alternative methods for dating ML phylogenies to be used for GMYC. Even when different

analyses indicated exactly the same number of species (e.g. nine species), the hypotheses were inconsistent for the haplotype composition of the candidate species. The oversplitting obtained from the *COI* also appears unrealistic, because it would imply the syntopic existence of morphologically cryptic species sharing weakly diverging mitochondrial haplotypes.

In contrast, some of the candidate species inferred by the ABGD, the ASAP and the tree-based methods on the mitochondrial genes could represent intraspecific divergent lineages. Genetic structuring between populations of animals with low vagility, such as strictly endogeic invertebrates, at a small spatial scale is expected and often observed within complex geographical settings (e.g. Avise, 2009; Català *et al.*, 2021). This could be the case, for example, of a putative lineage represented by the populations sampled from the Brescia, Garda and western Venetian Prealps, as indicated by several molecular analyses (i.e. ABGD and ASAP on both mitochondrial loci, PTP on *COI* and GMYC on 16S). However, morphological comparison between these populations did not reveal a geographical pattern of phenotypic divergence.

The documented syntopy of two genetically and phenotypically discrete groups of specimens, found together during a single day, can be explained most probably by the coexistence of two species. The alternative explanation (the existence of a genetically and phenotypically dimorphic population of a single species) is much less likely, because all the other 26 analysed populations were found to be both genetically and morphologically uniform and ascribable to one or the other of the two species. We acknowledge that distinguishing intraspecific lineages from species-level lineages is implicitly somewhat arbitrary, because of the expected continuity and heterogeneity of the speciation process (e.g. Zachos, 2016; Conix, 2019). Nevertheless, the co-occurrence of specimens unambiguously recognized in two discrete groups by both molecular and morphological analyses is generally deemed to represent an additional line of evidence for species-level separation (e.g. Padial *et al.*, 2010; Solís-Lemus *et al.*, 2015; Cadena *et al.*, 2018). Additional sampling and analyses will be required to estimate the frequency of hybridization (if any), to assess possible hybrid zones or to test for mechanisms of reproductive isolation (e.g. Dufresnes *et al.*, 2020). The two resulting species were also found to show slightly different climatic niches within the investigated area, although we could not use climatic variation of inhabited sites as further evidence for drawing an independent species delimitation hypothesis.

Under the two-species hypothesis, according to the rules of zoological nomenclature (ICZN, 1999) the name *Clinopodes carinthiacus* (Latzel, 1880) should be maintained as the valid name for the more widespread species featuring shorter coxosternal denticles and fewer legs on average. The holotype of *C. carinthiacus* is a female with 55 pairs of legs (Latzel, 1880), which corresponds to the modal value for the females of one of the two species, while falling outside the documented range of variation for the females of the other species (Fig. 4; Supporting Information, Table S8). The holotype was collected from an unknown locality in Carinthia (Latzel, 1880), which is closer to the known sites of the first species and much more distant from those of the second species (Fig. 1). In parallel, the name *Clinopodes strasseri* Verhoeff, 1938 (up to now considered a synonym of *C. carinthiacus*) should be recognized as the valid name for the more eastern species with longer denticles and more numerous pairs of legs on average. The three syntypes of *C. strasseri* (one male and two females) have relatively elongate forcipular denticles, which explains why they were originally classified by Verhoeff (1938) as a subspecies of a different species with long denticles, namely *Clinopodes rodnaensis* (Verhoeff, 1938), and have 57–59 pairs of legs, which fall within the known range for the species under consideration, but not for the other (Fig. 4; Supporting Information, Table S8). Two of the syntypes were collected from two localities in our study area (near Cavasso Nuovo, in the Carnic Prealps, and near Kanal, in the Julian Prealps), and both localities are not only within the known range of the more widespread species, but especially close to known sites of the other species (Fig. 1). Other names can be recognized as junior synonyms for *C. carinthiacus s.s.*, but none for *C. strasseri* (Supporting Information, Table S12).

INTRASPECIFIC DIVERSITY AT A FINE GEOGRAPHICAL SCALE

Unlike larger soil animals and many other regularly epigeic organisms, the strictly endogeic centipedes so far regarded as *C. carinthiacus* revealed fine-scale geographical variation, encompassing both genetic and morphological features, even between conspecific populations separated by only tens of kilometres, throughout an area characterized by complex environmental variation and biogeographical history. The high level of genetic differentiation is particularly evident in *COI*, which has been adopted almost universally as the marker of choice to investigate species diversity in animals and for which comparable estimates of variation are more abundant. *COI* has been adopted as the 'barcoding' gene in many initiatives aimed at documenting animal diversity at the species level and therefore it has also been used tentatively in small endogeic animals over the last decade (e.g. Del Latte *et al.*, 2015). In our study case, within a maximum geographical distance of ~600 km, we found an average intraspecific genetic distance of

7.6% and a maximum distance between conspecific populations of 12.1%.

Our investigation of the between-population morphological diversity within a single species (*C. carinthiacus s.s.*), by means of both linear (distance-based) and geometric (landmark-based) morphometrics, revealed small but significant differences between populations, even within a relatively restricted geographical range. For some characters, such differences could be explained by different local selective pressures. For instance, subtle differences in the shape and relative size of different parts of the feeding apparatus could have been driven by different prey spectra. However, knowledge on both functional and trophic ecology of centipedes is still insufficient to draw a realistic hypothesis (Bortolin *et al.*, 2018). Differences in the average number of pairs of legs could even be non-adaptive and explained by random drift.

FINAL REMARKS

The integrative taxonomic approach adopted here proved useful for drawing fairlywell supported, yet so far overlooked, species boundaries in small endogeic animals across a heterogeneous region. The methodology provided consistent results despite the relatively small number of specimens available, the substantial differentiation between and within populations, and the diverse pattern of variation among different biological features, including genetic and morphological traits. This is valuable, because these conditions are common in taxonomic studies on animals living their entire life in the soil matrix and especially in those showing low density and low probability of detection, such as endogeic geophilomorph centipedes.

ACKNOWLEDGEMENTS

DATA AVAILABILITY

All data are available from the authors upon request.

REFERENCES

Archidona-Yuste A, **Navas-Cortés JA**, **Cantalapiedra-Navarrete C**, **Palomares-Rius JE**, **Castillo P. 2016.** Unravelling the biodiversity and molecular phylogeny of needle nematodes of the genus *Longidorus* (Nematoda: Longidoridae) in olive and a description of six new species. *PLoS One* **11:** e0147689.

Avise JC. 2009. Phylogeography: retrospect and prospect. *Journal of Biogeography* **36:** 3–15.

Baiocco M, **Bonato L**, **Cardini A**, **Fusco G. 2017.** Shape variation of prey-catching structures in geophilomorph centipedes: a preliminary investigation using geometric morphometrics. *Zoologischer Anzeiger* **268:** 11–18.

Bardgett RD, **van der Putten WH. 2014.** Belowground biodiversity and ecosystem functioning. *Nature* **515:** 505–511.

Bates D, **Mächler M**, **Bolker B**, **Walker S. 2015.** Fitting linear mixed-effects models using lme4. *Journal of Statistical Software* **67:** 1–48.

Bedek J, **Taiti S**, **Bilandžija H**, **Ristori E**, **Baratti M. 2019.** Molecular and taxonomic analyses in troglobiotic *Alpioniscus* (*Illyrionethes*) species from the Dinaric Karst (Isopoda: Trichoniscidae). *Zoological Journal of the Linnean Society* **187:** 539–584.

Bedia J, **Herrera S**, **Gutiérrez JM. 2013.** Dangers of using global bioclimatic datasets for ecological niche modeling. Limitations for future climate projections. *Global and Planetary Change* **107:** 1–12.

Blonder B. 2016. Do hypervolumes have holes? *The American Naturalist* **187:** E93–E105.

Blonder B. 2018. *Hypervolume: high dimensional geometry and set operations using kernel density estimation, support vector machines, and convex hulls. R package version 2.0.12.* https://CRAN.R-project.org/package=hypervolume

Bonato L, **Corbetta A**, **Giovine G**, **Romanazzi E**, **Šunje E**, **Vernesi C**, **Crestanello B. 2018.** Diversity among peripheral populations: genetic and evolutionary differentiation of *Salamandra atra* at the southern edge of the Alps. *Journal of Zoological Systematics and Evolutionary Research* **56:** 533–548.

Bonato L, **Edgecombe GD**, **Lewis JGE**, **Minelli A**, **Pereira LA**, **Shelley RM**, **Zapparoli M. 2010.** A common terminology for the external anatomy of centipedes (Chilopoda). *ZooKeys* **69:** 17–51.

Bonato L, **Iorio E**, **Minelli A. 2011.** The centipede genus *Clinopodes* C. L. Koch, 1847 (Chilopoda, Geophilomorpha, Geophilidae): reassessment of species diversity and distribution, with a new species from the Maritime Alps (France). *Zoosystema* **33:** 175–205.

Bonato L, **Lopresti M**, **Minelli A**, **Cerretti P. 2014.** ChiloKey, an interactive identification tool for the geophilomorph centipedes of Europe (Chilopoda, Geophilomorpha). *ZooKeys* **443:** 1–9.

Bonato L, **Minelli A. 2014.** Chilopoda Geophilomorpha of Europe: a revised list of species, with taxonomic and nomenclatorial notes. *Zootaxa* **3770:** 1–136.

Bond JE, **Stockman AK. 2008.** An integrative method for delimiting cohesion species: finding the population–species interface in a group of Californian trapdoor spiders with

extreme genetic divergence and geographic structuring. *Systematic Biology* **57:** 628–646.

Bookstein FL. 1991. *Morphometric tools for landmark data. Geometry and biology*. Cambridge: Cambridge University Pres.

Bortolin F, **Fusco G**, **Bonato L. 2018.** Comparative analysis of diet in syntopic geophilomorph species (Chilopoda, Geophilomorpha) using a DNA-based approach. *Soil Biology and Biochemistry* **127:** 223–229.

Bouveyron C, **Brunet-Saumard C. 2014.** Model-based clustering of high-dimensional data: a review. *Computational Statistics & Data Analysis* **71:** 52–78.

Broennimann O, **Fitzpatrick MC**, **Pearman PB**, **Petitpierre B**, **Pellissier L**, **Yoccoz NG**, **Thuiller W**, **Fortin M-J**, **Randin C**, **Zimmermann NE**, **Graham CH**, **Guisan A. 2012.** Measuring ecological niche overlap from occurrence and spatial environmental data. *Global Ecology and Biogeography* **21:** 481–497.

Cadena CD, **Zapata F**, **Jiménez I. 2018.** Issues and perspectives in species delimitation using phenotypic data: Atlantean evolution in Darwin's finches. *Systematic Biology* **67:** 181–194.

Camargo A, **Sites JW. 2013.** Species delimitation: a decade after the Renaissance. In: Pavlinov I, ed. *The species problem. Ongoing issues*. New York: InTech, 225–247.

Cardini A. 2014. Missing the third dimension in geometric morphometrics: how to assess if 2D images really are a good proxy for 3D structures? *Hystrix: the Italian Journal of Mammalogy* **25:** 63–72.

Cardoso P, **Mammola S**, **Rigal F**, **Carvalho J. 2021.** *BAT: Biodiversity Assessment Tools. R package version 2.7.0*. https://CRAN.R-project.org/package=BAT

Carstens BC, **Pelletier TA**, **Reid NM**, **Satler JD. 2013.** How to fail at species delimitation. *Molecular Ecology* **22:** 4369–4383.

Castresana J. 2002. *GBLOCKS: selection of conserved blocks from multiple alignments for their use in phylogenetic analysis. Version 0.91b*. EMBL. http://molevol.cmima.csic.es/castresana/Gblocks.html

Català C, **Bros V**, **Castelltort X**, **Santos X**, **Pascual M. 2021.** Deep genetic structure at a small spatial scale in the endangered land snail *Xerocrassa montserratensis*. *Scientific Reports* **11:** 8855.

Conix S. 2019. Measuring evolutionary independence: a pragmatic approach to species classification. *Biology & Philosophy* **34:** 53.

Dayrat B. 2005. Towards integrative taxonomy. *Biological Journal of the Linnean Society* **85:** 407–415.

Del Latte L, **Bortolin F**, **Rota-Stabelli O**, **Fusco G**, **Bonato L. 2015.** Molecular-based estimate of species number, phylogenetic relationships and divergence times for the genus *Stenotaenia* (Chilopoda, Geophilomorpha) in the Italian region. *ZooKeys* **510:** 31–47.

De Queiroz K. 1998. The general lineage concept of species, species criteria, and the process of speciation: a conceptual unification and terminological recommendations. In: Howard DJ, Berlocher SH, eds. *Endless forms: species and speciation*. Oxford: Oxford University Press, 57–75.

De Queiroz K. 2007. Species concepts and species delimitation. *Systematic Biology* **56:** 879–886.

Derkarabetian S, **Hedin M. 2014.** Integrative taxonomy and species delimitation in harvestmen: a revision of the western North American genus *Sclerobunus* (Opiliones: Laniatores: Travunioidea). *PLoS One* **9:** e104982.

DeSalle R, **Egan MG**, **Siddal M. 2005.** The unholy trinity: taxonomy, species delimitation and DNA barcoding. *Philosophical Transactions of the Royal Society B: Biological Sciences* **360:** 1905–1916.

Di Cola V, **Broennimann O**, **Petitpierre B**, **Breiner FT**, **D'Amen M**, **Randin C**, **Engler R**, **Pottier J**, **Pio D**, **Dubuis A**, **Pellissier L**, **Mateo RG**, **Hordijk W**, **Salamin N**, **Guisan A. 2017.** ecospat: an R package to support spatial analyses and modeling of species niches and distributions. *Ecography* **40:** 774–787.

Dong J, **Fernández-Baca D**, **McMorris FR. 2010.** Constructing majority-rule supertrees. *Algorithms for Molecular Biology* **5:** 2.

Dufresnes C, **Pribille M**, **Alard B**, **Gonçalves H**, **Amat F**, **Crochet PA**, **Dubey S**, **Perrin N**, **Fumagalli L**, **Vences M**, **Martínez-Solano I. 2020.** Integrating hybrid zone analyses in species delimitation: lessons from two anuran radiations of the Western Mediterranean. *Heredity* **124:** 423–438.

Eberle J, **Warnock RC**, **Ahrens D. 2016.** Bayesian species delimitation in *Pleophylla* chafers (Coleoptera) – the importance of prior choice and morphology. *BMC Evolutionary Biology* **16:** 94.

Edgecombe GD, **Colgan DJ**, **Sharkey D. 2006.** Phylogeny and biogeography of the Australasian centipede *Henicops* (Chilopoda: Lithobiomorpha): a combined morphological and molecular approach. *Insect Systematics and Evolution* **37:** 241–256.

Edwards DL, **Knowles LL. 2014.** Species detection and individual assignment in species delimitation: can integrative data increase efficacy? *Proceedings of the Royal Society B: Biological Science* **281:** 20132765.

Emerson BC, **Cicconardi F**, **Fanciulli PP**, **Shaw PJ. 2011.** Phylogeny, phylogeography, phylobetadiversity and the molecular analysis of biological communities. *Philosophical Transactions of the Royal Society B: Biological Sciences* **366:** 2391–2402.

Espinasa L, **Bartolo ND**, **Centone DM**, **Haruta CS**, **Reddell JR. 2016.** Revision of genus *Texoreddellia* Wygodzinsky, 1973 (Hexapoda, Zygentoma, Nicoletiidae), a prominent element of the cave-adapted fauna of Texas. *Zootaxa* **4126:** 221–239.

Espinasa L, **Giribet G. 2009.** Living in the dark — species delimitation based on combined molecular and morphological evidence in the nicoletiid genus *Texoreddellia* Wygodzinsky, 1973 (Hexapoda: Zygentoma: Nicoletiidae) in Texas and Mexico. *Texas Memorial Museum Speleological Monographs* **7:** 87–110.

Ezard TH, **Pearson PN**, **Purvis A. 2010.** Algorithmic approaches to aid species' delimitation in multidimensional morphospace. *BMC Evolutionary Biology* **10:** 175.

Flot JF. 2015. Species delimitation's coming of age. *Systematic Biology* **64:** 897–899.

Folmer O, **Black M**, **Hoeh W**, **Lutz R**, **Vrijenhoek RC. 1994.** DNA primers for amplification of mitochondrial cytochrome *c* oxidase subunit I from diverse metazoan invertebrates. *Molecular Marine Biology and Biotechnology* **3:** 294–299.

Fontaneto D, **Flot JF**, **Tang CQ. 2015.** Guidelines for DNA taxonomy, with a focus on the meiofauna. *Marine Biodiversity* **45:** 433–451.

Fraley C, **Raftery AE. 2002.** Model-based clustering, discriminant analysis, and density estimation. *Journal of the American Statistical Association* **97:** 611–631.

Georgopoulou E, **Djursvoll P**, **Simaiakis SM. 2016.** Predicting species richness and distribution ranges of centipedes at the northern edge of Europe. *Acta Oecologica* **74:** 1–10.

Gouy M, **Guindon S**, **Gascuel O. 2010.** SeaView version 4: a multiplatform graphical user interface for sequence alignment and phylogenetic tree building. *Molecular Biology and Evolution* **27:** 221–224.

Guillot G, **Renaud S**, **Ledevin R**, **Michaux J**, **Claude J. 2012.** A unifying model for the analysis of phenotypic, genetic, and geographic data. *Systematic Biology* **61:** 897–911.

Guindon S, Dufayard JF, Lefort V, Anisimova M, Hordijk W, Gascuel O. 2010. New algorithms and methods to estimate maximum-likelihood phylogenies: assessing the performance of PhyML 3.0. *Systematic Biology* **59:** 307–321.

Gutiérrez-Gutiérrez C, **Cantalapiedra-Navarrete C**, **Remesal E**, **Palomares-Rius JE**, **Navas-Cortés JA**, **Castillo P. 2013.** New insight into the identification and molecular phylogeny of dagger nematodes of the genus *Xiphinema* (Nematoda: Longidoridae) with description of two new species. *Zoological Journal of the Linnean Society* **169:** 548–579.

Gutiérrez-Gutiérrez C, **Palomares-Rius JE**, **Cantalapiedra-Navarrete C**, **Landa BB**, **Esmenjaud D**, **Castillo P. 2010.** Molecular analysis and comparative morphology to resolve a complex of cryptic *Xiphinema* species. *Zoologica Scripta* **39:** 483–498.

Hadley A. 2008. *Combine ZP*. Available at: https://github.com/Vincentdecursay/CombineZP

Hammer O, **Harper DA**, **Ryan PD. 2001.** PAST: paleontological statistics software package for education and data analysis. *Palaeontologia Electronica* **4:** art. 4.

Hausdorf B. 2011. Progress toward a general species concept. *Evolution; international journal of organic evolution* **654:** 923–931.

Heethoff M, **Laumann M**, **Weigmann G**, **Raspotnig G. 2011.** Integrative taxonomy: combining morphological, molecular and chemical data for species delineation in the parthenogenetic *Trhypochthonius tectorum* complex (Acari, Oribatida, Trhypochthoniidae). *Frontiers in Zoology* **8:** 2.

Hijmans RJ, **Cameron SE**, **Parra JL**, **Jones PG**, **Jarvis A. 2005.** Very high resolution interpolated climate surfaces for global land areas. *International Journal of Climatology* **25:** 1965–1978.

Hoban S, **Dawson A**, **Robinson JD**, **Smith AB**, **Strand AE. 2019.** Inference of biogeographic history by formally integrating distinct lines of evidence: genetic, environmental niche and fossil. *Ecography* **42:** 1991–2011.

Inäbnit T, **Jochum A**, **Kampschulte M**, **Martels G**, **Ruthensteiner B**, **Slapnik R**, **Nesselhauf C**, **Neubert E. 2019.** An integrative taxonomic study reveals carychiid microsnails of the troglobitic genus *Zospeum* in the Eastern and Dinaric Alps (Gastropoda, Ellobioidea, Carychiinae). *Organisms Diversity & Evolution* **19:** 135–177.

ICZN. **1999.** *International code of zoological nomenclature*. Singapore: International Trust for Zoological Nomenclature. Available at: https://www.iczn.org/the-code/the-code-online/

Joshi J, **Edgecombe GD. 2018.** Molecular phylogeny and systematics of the centipede genus *Ethmostigmus* Pocock (Chilopoda: Scolopendromorpha) from peninsular India. *Invertebrate Systematics* **32:** 1316–1335.

Joshi J, **Karanth PK**, **Edgecombe GD. 2020.** The out-of-India hypothesis: evidence from an ancient centipede genus, *Rhysida* (Chilopoda: Scolopendromorpha) from the Oriental Region, and systematics of Indian species. *Zoological Journal of the Linnean Society* **189:** 828–861.

Kalyaanamoorthy S, **Minh BQ**, **Wong TK**, **Von Haeseler A**, **Jermiin LS. 2017.** ModelFinder: fast model selection for accurate phylogenetic estimates. *Nature Methods* **14:** 587–589.

Katoh K, **Standley DM. 2013.** MAFFT multiple sequence alignment software version 7: improvements in performance and usability. *Molecular Biology and Evolution* **30:** 772–780.

Klingenberg CP. 2011. MORPHOJ: an integrated software package for geometric morphometrics. *Molecular Ecology* **11:** 353–357.

Klingenberg CP, **Barluenga M**, **Meyer A. 2002.** Shape analysis of symmetric structures: quantifying variation among individuals and asymmetry. *Evolution; international journal of organic evolution* **56:** 1909–1920.

Kumar S, **Stecher G**, **Tamura K. 2016.** MEGA7: molecular evolutionary genetics analysis version 7.0 for bigger datasets. *Molecular Biology and Evolution* **33:** 1870–1874.

Latzel R. 1880. *Die Myriopoden der Österreichisch-Ungarischen Monarchie*. Vienna: Hölder.

Leigh JW, **Bryant D. 2015.** POPART: full-feature software for haplotype network construction. *Methods in Ecology and Evolution* **6:** 1110–1116.

Marazzi S. 2005. *Atlante Orografico delle Alpi. SOIUSA*. Turin: Priuli & Verlucca.

Marchán DF, **Fernández R**, **Domínguez J**, **Díaz Cosín DJ**, **Novo M. 2020.** Genome-informed integrative taxonomic description of three cryptic species in the earthworm genus *Carpetania* (Oligochaeta, Hormogastridae). *Systematics and Biodiversity* **18:** 203–215.

Marchán DF, **Fernández R**, **de Sosa I**, **Sánchez N**, **Díaz Cosín DJ**, **Novo M. 2018.** Integrative systematic revision of a Mediterranean earthworm family: Hormogastridae (Annelida, Oligochaeta). *Invertebrate Systematics* **32:** 652–671.

Margush T, **McMorris FR. 1981.** Consensus *n*-trees. *Bulletin of Mathematical Biology* **43:** 239–244.

Minelli A, **Koch M. 2011.** Chilopoda – general morphology. In: Minelli A, ed. *Treatise on zoology – anatomy, taxonomy, biology. The Myriapoda*, *Vol. 1*. Leiden: Brill, 43–66.

Mitteroecker P, **Bookstein F. 2011.** Linear discrimination, ordination, and the visualization of selection gradients in modern morphometrics. *Evolutionary Biology* **38:** 100–114.

Monaghan MT, **Wild R**, **Elliot M**, **Fujisawa T**, **Balke M**, **Inward DJG**, **Lees DC**, **Ranaivosolo R**, **Eggleton P**, **Barraclough TG**, **Vogler AP. 2009.** Accelerated species inventory on Madagascar using coalescent-based models of species delineation. *Systematic Biology* **58:** 298–311.

Murienne J, **Edgecombe GD**, **Giribet G. 2010.** Including secondary structure, fossils and molecular dating in the centipede tree of life. *Molecular Phylogenetics and Evolution* **57:** 301–313.

Nguyen LT, **Schmidt HA**, **Von Haeseler A**, **Minh BQ. 2015.** IQ-TREE: a fast and effective stochastic algorithm for estimating maximum-likelihood phylogenies. *Molecular Biology and Evolution* **32:** 268–274.

Noguerales V, **Cordero PJ**, **Ortego J. 2018.** Integrating genomic and phenotypic data to evaluate alternative phylogenetic and species delimitation hypotheses in a recent evolutionary radiation of grasshoppers. *Molecular Ecology* **27:** 1229–1244.

Nosil P, **Harmon LJ**, **Seehausen O. 2009.** Ecological explanations for (incomplete) speciation. *Trends in Ecology & Evolution* **24:** 145–156.

Ohira H, **Kaneko S**, **Faulks L**, **Tsutsumi T. 2018.** Unexpected species diversity within Japanese *Mundochthonius* pseudoscorpions (Pseudoscorpiones: Chthoniidae) and the necessity for improved species diagnosis revealed by molecular and morphological examination. *Invertebrate Systematics* **32:** 259–277.

Olson M, **Harris T**, **Higgins R**, **Mullin P**, **Powers K**, **Olson S**, **Powers TO. 2017.** Species delimitation and description of *Mesocriconema nebraskense* n. sp. (Nematoda: Criconematidae), a morphologically cryptic, parthenogenetic species from North American Grasslands. *Journal of Nematology* **49:** 42–66.

Orgiazzi A, **Bardgett RD**, **Barrios E**, **Behan-Pelletier V**, **Briones MJI**, **Chotte J-L**, **De Deyn GB**, **Eggleton P**, **Fierer N**, **Fraser T**, **Hedlund K**, **Jeffery S**, **Johnson NC**, **Jones A**, **Kandeler E**, **Kaneko N**, **Lavelle P**, **Lemanceau P**, **Miko L**, **Montanarella L**, **Moreira F**, **Ramirez KS**, **Scheu S**, **Singh BK**, **Six J**, **Van der Putten WH**, **Wall DH, eds. 2016.** *Global soil biodiversity atlas*. Luxembourg: European Commission, Publications Office of the European Union.

Padial JM, **Miralles A**, **De la Riva I**, **Vences M. 2010.** The integrative future of taxonomy. *Frontiers in Zoology* **7:** 16.

Pentinsaari M, **Vos R**, **Mutanen M. 2017.** Algorithmic single-locus species delimitation: effects of sampling effort, variation and nonmonophyly in four methods and 1870 species of beetles. *Molecular Ecology Resources* **17:** 393–404.

Peretti E, **Bonato L. 2018.** How many species of centipedes coexist in temperate forests? Estimating local species richness of Chilopoda in soil coenoses of the south-eastern Prealps. *European Journal of Soil Biology* **89:** 25–32.

Pérez-González S, **Andújar C**, **Lantero E**, **Zaballos JP. 2018.** On the verge of below-ground speciation: a new species complex of microendemic endogean carabid beetles, *Typhlocharis* Dieck, 1869 (Coleoptera: Carabidae: Anillini),

from south-west Iberian Peninsula. *Arthropod Systematics & Phylogeny* **76:** 429–447.

Pons J, **Barraclough TG**, **Gomez-Zurita J**, **Cardoso A**, **Duran DP**, **Hazell S**, **Kamoun S**, **Sumlin WD**, **Vogler AP. 2006.** Sequence-based species delimitation for the DNA taxonomy of undescribed insects. *Systematic Biology* **55:** 595–609.

Posada D. 2008. jModelTest: phylogenetic model averaging. *Molecular Biology and Evolution* **25:** 1253–1256.

Powers TO, **Bernard EC**, **Harris T**, **Higgins R**, **Olson M**, **Olson S**, **Lodema M**, **Matczyszyn J**, **Mullin P**, **Sutton L**, **Powers KS. 2016.** Species discovery and diversity in *Lobocriconema* (Criconematidae: Nematoda) and related plant-parasitic nematodes from North American ecoregions. *Zootaxa* **4085:** 301–344.

Puillandre N, **Brouillet S**, **Achaz G. 2021.** ASAP: assemble species by automatic partitioning. *Molecular Ecology Resources* **21:** 609–620.

Puillandre N, **Lambert A**, **Brouillet S**, **Achaz G. 2012.** ABGD, Automatic Barcode Gap Discovery for primary species delimitation. *Molecular Ecology* **21:** 1864–1877.

Richardson JL, **Urban MC**, **Bolnick DI**, **Skelly DK. 2014.** Microgeographic adaptation and the spatial scale of evolution. *Trends in Ecology & Evolution* **29:** 165–176.

Rohlf FJ. 2015. The tps series of software. *Hystrix: the Italian Journal of Mammalogy* **26:** 9–12.

Rohlf FJ, **Slice D. 1990.** Extensions of the Procrustes method for the optimal superimposition of landmarks. *Systematic Biology* **39:** 40–59.

Rota E, **Martinsson S**, **Erséus C**, **Petushkov VN**, **Rodionova NS**, **Omodeo P. 2018.** Green light to an integrative view of *Microscolex phosphoreus* (Dugès, 1837) (Annelida: Clitellata: Acanthodrilidae). *Zootaxa* **4496:** 175–189.

Rueffler C, **Van Dooren TJ**, **Leimar O**, **Abrams PA. 2006.** Disruptive selection and then what? *Trends in Ecology & Evolution* **21:** 238–245.

Scarpino SV. 2020. *Package 'multiDimBio'. CRAN*. Vienna: R Foundation for Statistical Computing.

Schlick-Steiner BC, **Steiner FM**, **Seifert B**, **Stauffer C**, **Christian E**, **Crozier RH. 2010.** Integrative taxonomy: a multisource approach to exploring biodiversity. *Annual Reviews of Entomology* **55:** 421–438.

Scrucca L, **Fop M**, **Murphy TB**, **Raftery AE. 2016.** mclust 5: clustering, classification and density estimation using Gaussian finite mixture models. *The R Journal* **8/1:** 205–233.

Solís-Lemus C, **Knowles LL**, **Ané C. 2015.** Bayesian species delimitation combining multiple genes and traits in a unified framework. *Evolution; international journal of organic evolution* **69:** 492–507.

Stefani F, **Gentilli A**, **Sacchi R**, **Razzetti E**, **Pellitteri Rosa D**, **Pupin F**, **Galli P. 2012.** Refugia within refugia as a key to disentangle the genetic pattern of a highly variable species: the case of *Rana temporaria* Linnaeus, 1758 (Anura, Ranidae). *Molecular Phylogenetics and Evolution* **65:** 718–726.

Štundlová J, **Šmíd J**, **Nguyen P**, **Šťáhlavský F. 2019.** Cryptic diversity and dynamic chromosome evolution in

Alpine scorpions (Euscorpiidae: *Euscorpius*). *Molecular Phylogenetics and Evolution* **134:** 152–163.

Sun X, **Zhang F**, **Ding Y**, **Davies TW**, **Li Y**, **Wu D. 2017.** Delimiting species of *Protaphorura* (Collembola: Onychiuridae): integrative evidence based on morphology, DNA sequences and geography. *Scientific Reports* **7:** 8261.

Talavera G, **Dinca V**, **Vila R. 2013.** Factors affecting species delimitations with the GMYC model: insights from a butterfly survey. *Methods in Ecology and Evolution* **4:** 1101–1110.

Tamura K, **Battistuzzi FU**, **Billing-Ross P**, **Murillo O**, **Filipski A**, **Kumar S. 2012.** Estimating divergence times in large molecular phylogenies. *Proceedings of the National Academy of Sciences of the United States of America* **109:** 19333–19338.

Trifinopoulos J, **Nguyen L-T**, **von Haeseler A**, **Minh BQ. 2016.** W-IQ-TREE: a fast online phylogenetic tool for maximum likelihood analysis. *Nucleic Acids Research* **44:** W232–W235.

Varela S, **Lima-Ribeiro MS**, **Terribile LC. 2015.** A short guide to the climatic variables of the last glacial maximum for biogeographers. *PLoS One* **10:** e0129037.

Verhoeff KW. 1938. Chilopoden-Studien zur Kenntnis der Epimorphen Zoologische Jahrbücher. *Abteilung für Systematik, Ökologie und Geographie der Tiere* **71:** 339–388.

Warren DL, **Glor RE**, **Turelli M. 2008.** Environmental niche equivalency versus conservatism: quantitative approaches to niche evolution. *Evolution; international journal of organic evolution* **62:** 2868–2883.

Will KW, **Mishler BD**, **Wheeler QD. 2005.** The perils of DNA barcoding and the need for integrative taxonomy. *Systematic Biology* **54:** 844–851.

Zachos FE. 2016. *Species concepts in biology*. Cham: Springer.

Zhang F, **Jantarit S**, **Nilsai A**, **Stevens MI**, **Ding Y**, **Satasook C. 2018.** Species delimitation in the morphologically conserved *Coecobrya* (Collembola: Entomobryidae): a case study integrating morphology and molecular traits to advance current taxonomy. *Zoologica Scripta* **47:** 342–356.

Zhang J, **Kapli P**, **Pavlidis P**, **Stamatakis A. 2013.** A general species delimitation method with applications to phylogenetic placements. *Bioinformatics* **29:** 2869–2876.

SUPPORTING INFORMATION

Additional Supporting Information may be found in the online version of this article at the publisher's web-site:

Table S1. Position of the sampling sites for the integrative species delimitation analysis. Sites are ordered approximately from west to east. The elevation is approximated to the nearest 10 m a.s.l., and the geographical coordinates are approximated to the fifth decimal digit (~0.1 km).
Table S2. Specimens used for the integrative species delimitation analysis and haplotypes of the three genes. Sites are ordered approximately from west to east.
Table S3. Morphological characters analysed for within-population variation in relation to body size and sex and for between-population variation. Characters are ordered from anterior to posterior. Operational definitions of distance measurements are given in the Supporting Information (Table S4). For characters defined on paired symmetrical structures, we considered the left side whenever it was not damaged or obviously anomalous. The ten characters used in the species delimitation analysis are highlighted.
Table S4. Operational definitions of distance measurements, ordered from anterior to posterior. Some distance measurements are illustrated in the Supporting Information (Fig. S1).
Table S5. Pairwise Pearson correlation indexes between the bioclimatic variables in the study area. Variables BIO3, BIO14 and BIO15 were not considered (see Material and Methods). The variables used in the analysis are highlighted, and their correlations are in bold.
Table S6. Landmarks and semilandmarks used for the geometric morphometric analysis of intraspecific between-population variation of the shape of the forcipular coxosternite in *Clinopodes carinthiacus s.s.* (see also Fig. 6).
Table S7. Within-population variation of morphological characters in relation to body size and sex, assessed in 48 specimens from three sites through linear mixed models or generalized linear mixed models, with body size and sex as fixed effects and site as a random effect. Characters are ordered from anterior to posterior (for definitions, see Supporting Information, Tables S3 and S4). Measurements are in millimetres. Coefficients are in bold when estimated with statistical significance $P < 0.01$.
Table S8. Differences between the two resulting species in the number of pairs of legs, considering specimens identified confidently as belonging to the two species in the study area.
Table S9. Median and range of variation (minimum/maximum) of the climatic conditions in the sites of the two species.
Table S10. Results of MANOVA of 23 distance measurements between eight populations of the species *Clinopodes carinthiacus s.s.* (*N* = 40 females > 15 mm long). Characters are described in the Supporting Information (Table S4).

Table S11. Results of geometric morphometric analysis of the shape of the forcipular coxosternites (17 landmarks and semilandmarks; 40 specimens from eight populations of *Clinopodes carinthiacus s.s.*).

Table S12. Taxonomic names introduced in the past for specimens of *Clinopodes* from the study area or surrounding regions. Names are ordered according to the year of valid publication (ICZN, 1999). For names indicated with uncertainty as synonyms, further investigations outside the study area are needed to clarify the species identity of all type specimens.

Table S13. Differences between the two resulting species in selected morphological characters.

Figure S1. Distance measurements taken on a representative specimen of *Clinopodes carinthiacus* (PD-G 7787 from Mt Cesen, eastern Venetian Prealps). Measure codes are as in the Supporting Information (Table S4).

Figure S2. Haplotype networks of 16S (58 specimens from 26 sites; median-joining network), *COI* (56 specimens from 25 sites; TCS network) and 28S (54 specimens from 25 sites; median-joining network). Colour codes refer to the sites as indicated on the map.

Figure S3. Left: number of candidate species suggested by automatic barcode gap discovery (ABGD) in relation to prior maximum intraspecific divergence (P), before collapsing to one species. Yellow lines represent the number of species indicated by the initial analysis; red lines represent the number of species indicated by the recursive analysis. Right: partitions in candidate species proposed by assemble species by automatic partitioning (ASAP) for the three genes.

Figure S4. Maximum likelihood tree of the 25 unique combinations of haplotypes of the three genes (16S, *COI* and 28S) and their subdivision into candidate species according to Poisson tree process (PTP; numbers indicate support values for the candidate species). The subdivisions obtained by the PTP analyses of the single genes 16S and *COI* are indicated for comparison (see Fig. 2). Mountain ranges where the haplotypes were found are also indicated.

Figure S5. Observed value (red line) and expected distribution under the hypothesis of niche equivalency (grey histogram) for Schoener's *D* index of niche overlap between the two resulting species, based on: A, 106 sites of *Clinopodes carinthiacus s.s.* and 16 sites of *Clinopodes strasseri* (precision of geolocalization ≤ 1 km); and B, 95 sites of *C. carinthiacus s.s.* and 13 sites of *C. strasseri* (precision of geolocalization ≤ 10 m).

Figure S6. Three-dimensional hypervolumes of the climatic niche of *Clinopodes carinthiacus s.s.* (green) and *Clinopodes strasseri* (red). Small circles are 10 000 random points sampled from each hypervolume for illustrative purposes. Large circles represent the centroid of each hypervolume.

Figure S7. Between-group principal components analysis of the symmetric component of the variation in shape of the forcipular coxosternite between eight populations of *Clinopodes carinthiacus s.s.*: distribution of 40 specimens on the first and third principal components. Polygons indicate populations (codes as in Table 1); wireframes along the axes represent the variation in shape (dark blue) compared with the average shape (light blue).